TASK 7 DEMONSTRATION OF STADIUM® FOR THE PERFORMANCE ASSESSMENT OF CONCRETE LOW ACTIVITY WASTE STORAGE STRUCTURES

Cementitious Barriers Partnership

March 2010

CBP-TR-2010-007-C3, Rev. 0

CEMENTITIOUS BARRIERS PARTNERSHIP TASK 7 DEMONSTRATION OF STADIUM® FOR THE PERFORMANCE ASSESSMENT OF CONCRETE LOW ACTIVITY WASTE STORAGE STRUCTURES

Eric Samson
SIMCO Technologies, Inc.
Québec, Canada

March 2010

CBP-TR-2010-007-C3, Rev. 0

ACKNOWLEDGEMENTS

This report was prepared for the United States Department of Energy in part under Contract No. DE-AC09-08SR22470 and is an account of work performed in part under that contract. Reference herein to any specific commercial product, process, or service by trademark, name, manufacturer, or otherwise does not necessarily constitute or imply endorsement, recommendation, or favoring of same by Savannah River Nuclear Solutions or by the United States Government or any agency thereof. The views and opinions of the authors expressed herein do not necessarily state or reflect those of the United States Government or any agency thereof. The authors would like to acknowledge the contributions of Elmer Wilhite of Savannah River National Laboratory, David Kosson of Vanderbilt University and CRESP, Jake Philip of the U.S. Nuclear Regulatory Commission, and Ed Garboczi of the National Institute of Standards and Technology for contributions to the document. They would also like to acknowledge the contributions of Media Services of Savannah River Nuclear Solutions and Savannah River National Laboratory personnel for editing and assistance with production of the document.

and

This report is based on work supported by the U. S. Department of Energy, under Cooperative Agreement Number DE-FC01-06EW07053 entitled 'The Consortium for Risk Evaluation with Stakeholder Participation III' awarded to Vanderbilt University. The opinions, findings, conclusions, or recommendations expressed herein are those of the author(s) and do not necessarily represent the views of the U.S. Department of Energy or Vanderbilt University.

DISCLAIMER

Printed in the United States of America

United States Department of Energy
Office of Environmental Management
Washington, DC

This document is available on the U.S. DOE Information Bridge and on the CBP website: http://cementbarriers.org/
An electronic copy of this document is also available through links on the following websites: http://srnl.doe.gov/ and http://cementbarriers.org/

FOREWORD

The Cementitious Barriers Partnership (CBP) Project is a multi-disciplinary, multi-institutional collaboration supported by the United States Department of Energy (US DOE) Office of Waste Processing. The objective of the CBP project is to develop a set of tools to improve understanding and prediction of the long-term structural, hydraulic, and chemical performance of cementitious barriers used in nuclear applications.

A multi-disciplinary partnership of federal, academic, private sector, and international expertise has been formed to accomplish the project objective. In addition to the US DOE, the CBP partners are the Savannah River National Laboratory (SRNL), Vanderbilt University (VU) / Consortium for Risk Evaluation with Stakeholder Participation (CRESP), Energy Research Center of the Netherlands (ECN), and SIMCO Technologies, Inc. The Nuclear Regulatory Commission (NRC) is providing support under a Memorandum of Understanding. The National Institute of Standards and Technology (NIST) is providing research under an Interagency Agreement. Neither the NRC nor NIST are signatories to the CRADA.

The periods of cementitious performance being evaluated are >100 years for operating facilities and > 1000 years for waste management. The set of simulation tools and data developed under this project will be used to evaluate and predict the behavior of cementitious barriers used in near-surface engineered waste disposal systems, e.g., waste forms, containment structures, entombments, and environmental remediation, including decontamination and decommissioning analysis of structural concrete components of nuclear facilities (spent-fuel pools, dry spent-fuel storage units, and recycling facilities such as fuel fabrication, separations processes). Simulation parameters will be obtained from prior literature and will be experimentally measured under this project, as necessary, to demonstrate application of the simulation tools for three prototype applications (waste form in concrete vault, high-level waste tank grouting, and spent-fuel pool). Test methods and data needs to support use of the simulation tools for future applications will be defined.

The CBP project is a five-year effort focused on reducing the uncertainties of current methodologies for assessing cementitious barrier performance and increasing the consistency and transparency of the assessment process. The results of this project will enable improved risk-informed, performance-based decision-making and support several of the strategic initiatives in the DOE Office of Environmental Management Engineering & Technology Roadmap. Those strategic initiatives include 1) enhanced tank closure processes; 2) enhanced stabilization technologies; 3) advanced predictive capabilities; 4) enhanced remediation methods; 5) adapted technologies for site-specific and complex-wide D&D applications; 6) improved SNF storage, stabilization and disposal preparation; 7) enhanced storage, monitoring and stabilization systems; and 8) enhanced long-term performance evaluation and monitoring.

Christine A. Langton, PhD
Savannah River National Laboratory

David S. Kosson, PhD
Vanderbilt University / CRESP

EXECUTIVE SUMMARY

This report summarizes the simulation results obtained with the model STADIUM® for typical Cementitious Barrier Partnership (CBP) problems. The model was used to simulate the transport of ions from the pore solution of a salt waste form surrogate material through a concrete barrier in order to estimate the long-term durability of low activity waste storage structures. The simulations were performed before improvements to STADIUM® planned in the CBP research program were completed. Accordingly, the version of the model used in Task 7 could not predict the formation of cracks due to the presence of expansive sulfate-bearing minerals in the hydrated cement paste.

Simulations were performed to estimate the long term impact of several factors: thickness of the waste form material, flow field around the concrete barrier, finite element mesh density, concrete transport properties and initial mineral assemblage in the waste form material. The simulations were performed with transport properties estimated from laboratory tests performed on concretes corresponding to the Vault 1/4 and Vault 2 mixtures. The properties of the waste form were also obtained from laboratory experiments.

The calculations made in this report showed the capacity of STADIUM® in handling complex multilayer cases to predict the durability of concrete barriers in contact with sulfate bearing Saltstone-type material. The results highlighted important factors to consider in long-term analyses. For instance, the thickness of the Saltstone layer considered in the simulation has a significant impact on the model prediction. The results obtained in this report indicate that at least 3 m of salt waste material should be used to simulate the long term durability of the barrier.

At the soil/concrete barrier interface, the simulations indicated that the thickness of the soil layer considered has very little impact on the kinetics of the ettringite front penetration that starts at the Saltstone/concrete boundary. The soil layer does have an influence on the rate of decalcification of C-S-H at the soil/concrete barrier interface.

However, the most important result concerns the influence of different mineral assemblages in the Saltstone mixture. One set of minerals used for the simulations did not initiate the penetration of an ettringite front in the concrete barrier despite the high sulfate concentration in the pore solution. The absence of ettringite means that the concrete is not subject to sulfate attack and could prove highly durable for an extensive period of time. This surprising result emphasizes the need for experimental research work in order to have a better understanding of the complex interaction between the salt waste material and the concrete barrier.

CONTENTS

LIST OF FIGURES

LIST OF TABLES

LIST OF SYMBOLS

a, b, c, d	fitting parameters
h	heat exchange coefficient
H	hydration function
L	Dimension of the space domain
m	mesh refinement parameter
n	number of a node in a 1D FE mesh
n_o	number of the first node in a 1D FE mesh
N	total number of node in a FE mesh
q	heat flux
t	time
t^{ref}	curing time at which transport properties were measured
T	temperature
T_∞	outside (environment) temperature
α	rate of the time evolution of transport properties, due to hydration
γ	specific gravity
κ	intrinsic permeability
τ	intrinsic tortuosity
ξ	reference space [0...1]

LIST OF ACRONYMS AND ABBREVIATIONS

1D	One dimension
CBP	Cementitious Barrier Partnership
CPU	Central Processing Unit
C-S-H	Calcium Silicate Hydrates
FE	Finite Element
FEM	Finite Element Method
RH	Relative Humidity
SRS	Savannah River Site
w/b	water-to-binder ratio
w/c	water-to-cement ratio

CBP TASK 7 DEMONSTRATION OF STADIUM® FOR THE PERFORMANCE ASSESSMENT OF CONCRETE LOW ACTIVITY WASTE STORAGE STRUCTURES

Eric Samson
SIMCO Technologies, Inc.
Québec, Canada

1.0 INTRODUCTION

The objective of Task 7 is to show the calculations that can be performed with the current version of STADIUM® for typical Cementitious Barrier Partnership (CBP) problems. The model was used to simulate the transport of ions from the pore solution of a salt waste form surrogate material ("Saltstone" hereafter) through a concrete barrier in order to estimate the long-term durability of low activity waste storage structures. The test cases described in this document were inspired by the paper *Reference Cases for Use in the Cementitious Barriers Partnership* presented at the Waste Management conference in March 2009 and materials and conditions associated with the Savannah River Site (SRS) Saltstone Disposal Facility (SIMCO 2009a, SIMCO 2009b).

The complexity of the Saltstone/concrete barrier/soil system offers many technical difficulties to modelers. The physical and chemical phenomena involved largely contribute to the challenges of the problem. Also, performing the simulations over a period of 10,000 years makes computation time management part of the problem. The simulations were performed to show the ability of STADIUM® to predict the formation of deleterious phases like ettringite in the concrete barrier. Simulations were also performed to provide meaningful and useful ways to simplify the problem and assist engineers and scientists doing the performance assessment of the waste disposal facilities.

2.0 DEMONSTRATION CASE DESCRIPTION

The test cases are illustrated in Figure 1. The objective of the simulations is to estimate the durability of a 20-cm concrete layer that acts as a barrier to prevent the leaching of contaminants to the soil from the Saltstone slurry. The main concern is the presence of sulfate ions in the slurry. Due to concentration gradients, the ions may diffuse from the slurry into the concrete. Upon sulfate penetration, there is a risk that deleterious phases such as ettringite can precipitate and damage the barrier.

Figure 1a illustrates the most complete test case. It consists in a layer of concrete in contact with Saltstone on one side and soil on the other side. As mentioned previously, the concrete layer has a 20-cm thickness. The thickness of the Saltstone layer can exceed 6 m. Simulating such a large amount of material has significant impact on the calculation time. The first series of simulations investigates the effect of the Saltstone layer

thickness on the simulation results. The objective is to determine the minimum thickness that is required to represent a semi-infinite amount of Saltstone. For these simulations, it is assumed that the flow field in the soil is large. This case corresponds to the walls of a storage facility. In this case, it is possible to neglect the soil layer and assume zero concentrations for the main species considered (see Figure 2a). This corresponds to the case illustrated in Figure 1b. Simulations were performed with 50, 100, 200, 300 and 500 cm of Saltstone. The information collected from these simulations provides information that can be used to simplify the simulation process for performance assessment and consider only the concrete layer (Figure 1c).

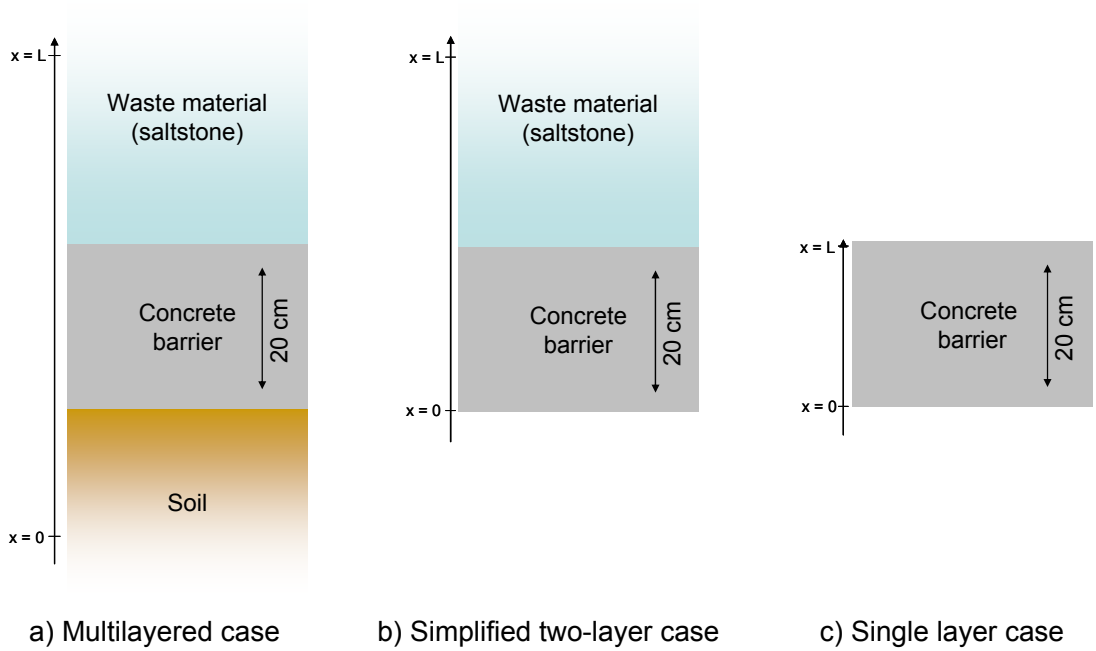

a) Multilayered case b) Simplified two-layer case c) Single layer case

Figure 1 – Schematic representation of demonstration cases

The next series of simulations was performed to investigate the impact of different soil layers on the durability of the concrete barrier. Simulations with 1 m and 3 m of soil were simulated, with zero concentration imposed at the end of the soil layer. This is similar to considering different flow fields around the storage structure (Figure 2). The simulation results were compared to the case without a soil layer.

In order to keep the calculation time as low as possible without affecting the quality of the numerical solutions, simulations were performed to investigate the effect of the mesh density. This parameter is also very critical to computation time and will be especially important if statistical analysis is performed with STADIUM®.

Another series of simulations was concerned with the concrete mixture properties. A simulation was performed with the transport properties of a second concrete mixture and compared to the results of previous simulations. The concrete mixture properties are detailed in the next section.

Finally, a simulation investigated the effect of the mineral phase assemblage in the Saltstone on the long-term durability. This simulation showed that depending on the initial set of minerals in the Saltstone slurry,

ettringite may or may not form in the concrete layer. This finding clearly suggests that the experimental characterization of Saltstone is key to the durability analyses.

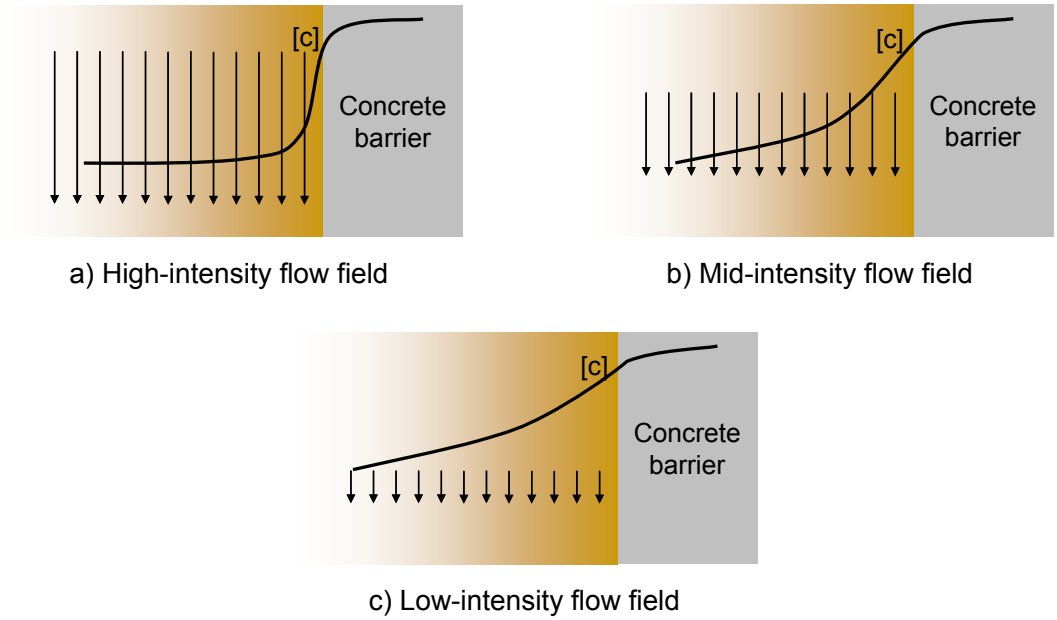

Figure 2 – Effect of flow field intensity on concentration in soil

All simulations were performed at 15°C. STADIUM® offers the possibility of simulating time-dependent boundary conditions so a more realistic external temperature could be simulated. However, it is important to note that time-dependent boundary conditions make it difficult to use an adaptive time-stepping scheme to speed up the simulation process. Given the 10,000-year time scale, this can become a serious concern. The adaptive time-stepping functions in STADIUM® were used for all the simulations presented in this report. Details are provided later.

Similarly, the simulations were all performed for saturated conditions. The previous comments apply here for time-dependent moisture boundary conditions. The situation may even prove more critical since unsaturated conditions are very likely to make convergence difficult due to the very different moisture characteristics of the concrete and the Saltstone. This was not tested in the present report.

All simulations were performed in one dimension (1D) over 10,000 years.

3.0 MATERIAL PROPERTIES

The properties were estimated on materials similar to those described in the paper *Reference Cases for Use in the Cementitious Barriers Partnership.* Samples were prepared by SIMCO Technologies Inc. and tested to get the main transport properties: porosity, tortuosity (diffusion coefficients), desorption isotherm and moisture

transport properties. The moisture transport properties are expressed as a permeability or using an empirical moisture diffusivity based on an exponential relationship.

3.1. Concrete Barrier

Two different concrete mixtures were used for the simulations. The SRS Vault 1/4 mixture was made with Type I/II cement (60%) and slag (40%) at a water-to-binder ratio of 0.38. The SRS Vault 2 material is a quaternary mixture incorporating Type V cement (30%), slag (40%), Type F fly ash (23%) and silica fume (7%) prepared at a 0.38 water-to-binder ratio. The materials were cured in a fog room before being tested at different curing intervals. The chemical composition of the cementitious materials is provided in Table 1. The properties of both mixtures are summarized in Table 2.

Table 1 – Chemical and physical characteristics of binders

Oxides (%mass)	Type I/II cement	Type V cement	Slag	Silica fume	Class F Fly Ash
CaO	64.3	63.0	35.8	0.50	1.41
SiO_2	21.0	20.8	39.1	96.6	53.1
Al_2O_3	4.91	4.11	10.1	0.21	28.4
Fe_2O_3	3.50	4.32	0.36	0.18	7.99
SO_3	2.64	2.36	1.99	<0.1	<0.10
MgO	0.95	2.40	12.6	0.28	1.00
K_2O	0.37	0.57	0.27	0.50	2.99
Na_2O	0.09	0.07	0.22	0.07	0.44
LOI	1.32	1.73	0	1.21	2.39
Specific gravity (–)	3.27	3.29	2.99	2.32	2.36

Table 2 lists two values for the porosity. Measurements made at SIMCO following the ASTM C642 standard procedure showed that this method can underestimate porosity values for high performance materials. An alternate method based on the water retention (desorption) measurements provided more realistic values. Consequently, the simulations were performed with the desorption test values.

Other properties are estimated from the measured properties and used as input to STADIUM®. To take into account the reduction in transport properties due to the hydration process, the tortuosity values are fitted to the function:

$$H(t) = \frac{a}{1 + (a-1)e^{-\alpha(t-t^{\mathrm{ref}})}} \qquad (1)$$

to determine the parameters a and α at the reference time t^{ref} (taken here as 28 days). This function multiplies the tortuosity in STADIUM® to yield a corrected diffusion coefficient. Using the data in Table 2, the values of

a and α for the Vault 1/4 mixture are 1.0 and 0.0 respectively, indicating a stable tortuosity through time. For the Vault 2 mixture, a=0.8 and α=0.015 1/s.

The initial mineral assemblage of the hydrated cement paste is calculated on the basis of the mixture proportions and chemical composition of the cementitious materials, as given in Table 1. Depending on the relative amount of sulfur and alumina, the hydrated system includes monosulfate and ettringite or monosulfate and hydroxy-AFm (C_4AH_{13}). The complete calculation method is detailed in Appendix A. The values for each concrete mixture are given in Table 3.

To estimate the initial pore solution, the measured concentrations of OH^-, Cl^-, Na^+ and K^+ are provided to STADIUM®. The values are adjusted proportionally to their mass fraction in the solution in order to meet the electroneutrality requirement. The concentrations in calcium, alumina and silica are calculated during the first time step in order to be in equilibrium with the minerals listed in Table 3.

3.2. Saltstone Mixture

A single salt waste form ("Saltstone") mixture was used for the simulations. The properties were obtained from Saltstone slurry prepared at a water-to-binder ratio of 0.6 with Type I/II cement, slag and fly ash. The paste was prepared with the high pH mixing solution detailed in Table 4. Samples were cast in cylinders for transport properties measurements and in cubic molds for compressive strength measurements. For the initial curing phase, the samples were kept in molds and placed under a plastic sheet in the laboratory. Wet burlap was placed beside the samples under the plastic sheet to maintain high relative humidity (RH) conditions. When the slurry was set, the molds were covered with wet burlap without marring the top surface of the material and placed under a plastic sheet. After three days, the molds (cylinders and cubes) were sealed in plastic bags and placed in a moist room (100% RH). Samples were taken out of the plastic bags at different time intervals for testing following the procedures described previously for the concrete mixtures. The properties of the Saltstone mixture are summarized in Table 5. The chemical composition of the cementitious materials is provided in Table 1.

Similar to the concrete mixtures, a function (Eq. (1)) is used to model the effect of the hydration process on the transport properties. In the case of the Saltstone, the measurements give the following values: a=0.3 and α=0.003 1/s.

The properties of the waste form given in Table 5 reflect the particular composition of this material. Similar to a hydrated cement paste prepared a high water to cement ratio (w/c) (Maltais 2004), the waste form paste exhibits a high porosity. But the presence of slag, silica fume and fly ash lowers the tortuosity, so that the slurry has characteristics that a similar to those of a low w/c material. In the case of permeability, this parameter is directly linked to the porosity. Accordingly, it is much higher than the permeability of the Vault 1/4 and Vault 2 mixtures.

Table 2 – Properties of vault concretes

Properties	Units	Concrete mixtures	
		Vault 1/4	Vault 2
Water/binder ratio		0.38	0.38
Cement type	(-)	I/II	V
Cement	(kg/m^3)	255	121
Mineral admixture	(kg/m^3)		
GGBFS		169	162
Fly ash (F)			95
Silica fume			27
Water	(kg/m^3)	162	152
Fine aggregate	(kg/m^3)	691	548
Coarse aggregate	(kg/m^3)	1096	1111
Compressive strength	(MPa)		
7d		42.7	41.6
28d		54.0	56.7
91d		65.3	62.1
Porosity (ASTM C642)	(% vol.)		
28d		10.0	10.3
91d		10.5	10.6
Porosity (Desorption Test)			
91d		12.0	13.5
Pore solution @ 28d	(mmol/L)		
OH^-		420	400
Na^+		231	287
K^+		252	142
Cl^-		0	5
Water content (desorp.) vs RH after 91d of hydration	(m^3/m^3)		
97.3 %		0.112	0.121
94.6 %		0.108	0.122
91.0 %		0.108	0.125
85.1 %		0.106	0.122
75.5 %		0.099	0.111
54.4 %		0.081	0.075
33.1 %		0.051	0.038
11.3 %		0.031	0.021
Tortuosity	(-)		
28d		0.0069	0.0027
91d		0.0070	0.0023
Water diffusivity (28d)			
A	(10^{-14} m^2/s)	0.02	1.2
B	(-)	112.0	67.6
Permeability	(10^{-22} m^2)	5.0	18.0

Table 3 – Initial minerals in the hydrated materials

Initial Mineral Assemblage ($g/kg_{material}$)	Concrete Mixture	
	Vault 1/4	Vault 2
C-S-H	102.1	51.5
Portlandite	2.2	0.0
Monosulfate	29.8	19.4
C_4AH_{13}	7.3	14.8

Table 4 – Saltstone mixing solution

Chemicals	M.M.	(mmol/L of DI Water)	(g/L of DI Water)	(mmol/L of Solution)
NaOH	39.99734	1590	63.6	1381
$NaNO_3$	84.9949	3160	268.58	2745
$NaNO_2$	68.9955	370	25.53	321
Na_2CO_3	105.9889	180	19.08	156
Na_2SO_4	142.0426	60	8.52	52
$Al_3(NO_3)_3$ ($9H_2O$)	429.09522	50	21.45	43
Na_3PO_4 ($12H_2O$)	388.124721	10	3.8	9
TOTAL			410.56	

Table 5 – Properties of the Saltstone mixture

Properties	Units	Saltstone mixture
Water/binder ratio		0.595
Cement type	(-)	I/II
Cement	(kg/m^3)	135
Mineral admixtures	(kg/m^3)	
GGBFS		195
Fly ash (F)		600
Silica fume		-
DI Water	(kg/m^3)	553
Salts	(kg/m^3)	227
Fine aggregate	(kg/m^3)	-
Coarse aggregate	(kg/m^3)	-
Compressive strength	(MPa)	
7d		2.1
28d		3.2
123d		4.0
Porosity	(% vol.)	
82d		65.3
123d		64.5
Pore solution @ 28d	(mmol/L)	
OH^-		485
Na^+		4420
K^+		119
SO_4^{2-}		120
Cl^-		9
N (NO_2^- + NO_3^-)		3576
CO_3^{2-}		115
Tortuosity	(–)	
28d		0.0142
123d		0.0133
Water content (desorp.) vs RH after 2 months of hydration	(m^3/m^3)	
97.3 %		0.615
94.6 %		0.501
91.0 %		0.407
85.1 %		0.319
75.5 %		0.237
54.4 %		0.162
33.1 %		0.114
11.3 %		0.078
Water diffusivity (@ 28d)		
A	(10-14 m^2/s)	92
B	(-)	10
Permeability	(10^{-22} m^2)	4000

The calculation of the initial phase assemblage for Saltstone is complicated by the highly charged mixing solution. To estimate the initial set of hydration products, it is assumed that the species in the mixing solution are all available for hydration. Also, the calculations are made assuming that the alkalis (Na^+, K^+) and nitrate/nitrite (NO_2^-, NO_3^-) do not react and are found in the pore solution[1]. From the mixing solution and the cementitious binder's chemical composition and proportions, the total amount of calcium, silica, alumina, sulfur and carbonate are calculated. From there, an initial assemblage of C-S-H, ettringite and calcite is assumed. These minerals and the measured concentrations in Na^+, K^+, NO_2^-, NO_3^-, and Cl^- are used as input[2] in the chemical equilibrium function of STADIUM® to get the mineral assemblage in the Saltstone slurry. The results are given in Table 6.

Table 6– Initial mineral assemblage in the Saltstone paste

Phases	Amount	
Minerals	($g/kg_{Saltstone}$)	
C-S-H	140.4	
Portlandite	4.9	
Ettringite	28.6	
Monocarboaluminate	11.0	
Calcite	4.8	
Pore solution	(mmol/L)	Act. coef.
OH^-	670.0	0.9236
Na^+	4420.0	0.4329
K^+	120.0	0.3145
SO_4^{2-}	130.7	0.0328
Ca^{2+}	0.41	0.0476
$Al(OH)_4^-$	0.14	0.6937
Cl^-	9.0	0.8100
$H_2SiO_4^{2-}$	9.7	0.0367
NO_3^-	2000.0	0.3953
NO_2^-	1575.0	0.3261
CO_3^{2-}	2.9	0.0599

[1] The concentration values for these species were measured from pore solution extraction (Table 5) and closely match the values found in the mixing solution.

[2] OH^- is also provided in order to have a neutral solution.

3.3. Soil Properties

Since STADIUM® does not contain the typical reaction mechanisms found in soils, this layer will be modeled as a nonreactive porous material that will only absorb ions leaching out of the concrete layer. The transport properties of the soil are arbitrarily set to a porosity of 35% and a tortuosity of 0.1.

The inputs to STADIUM® include the water to binder ratio, binder density, and the amounts of aggregate. To simulate the soil, a saturated wet density of 2650 kg/m^3 was targeted, along with a fictitious paste volume of 0.41. This value was selected because the damage function of STADIUM® then matches with the Kozeny-Carman relationship, which is commonly used to model feedback effects in soil. In order to meet these targets, the binder content was set to 1291.5 kg/m^3 (γ=3.15) and the aggregate content set to 1358.5 kg/m^3, with a water to binder ratio set to zero.

The ionic concentrations of all species as well as the mineral contents were set to zero at the start of the calculations. Even though the soil is not reactive, minerals are allowed to precipitate if the ionic activity product of a phase exceeds its equilibrium constant. Also, the presence of species in natural groundwater like sulfate and carbonate can be provided to STADIUM®. The zero concentration case was selected to estimate the long-term decalcification of the barrier.

4.0 NUMERICAL PARAMETERS

4.1. Chemical Data

There are eleven ionic species considered in the calculations: OH^-, Na^+, K^+, SO_4^{2-}, Ca^{2+}, $Al(OH)_4^-$, Cl^-, $H_2SiO_4^{2-}$, NO_2^-, NO_3^-, and CO_3^{2-}. All the chemical equilibrium expressions detailed in the next paragraphs are expressed in terms of these eleven main species.

The minerals that will be considered for the durability analysis are listed in Table 7. The portlandite, C-S-H, monosulfates, and C_4AH_{13} can be present initially in the cementitious materials (e.g., Table 3). The other minerals are phases that can be considered as possible precipitates due to the presence of SO_4^{2-} and other species in the pore solution.

The chemical equilibrium of C-S-H will be modeled on the basis of Berner's approach, which assumes that the mineral can be represented by a mixture of portlandite and CaH_2SiO_4. The model assigns separate C/S-dependent equilibrium relationships to the $Ca(OH)_2$ and CaH_2SiO_4 fractions. Based on this approach, it is possible to reproduce the incongruent behavior of C-S-H, as shown on Figure 3. Assuming that the C-S-H initially has a C/S ratio of 1.65, the initial amount of portlandite considered in the calculations represents the sum of the "real" portlandite and a contribution corresponding to 26.4% of the mass of the C-S-H is added. The remainder of the C-S-H, i.e., 73.6%, corresponds to CaH_2SiO_4.

Table 7 – Mineral phases considered for the calculations

Minerals	Composition	log(K_{sp}) @ 25°C
Portlandite†	$Ca(OH)_2$	-5.15 if C/S > 1.65 f(C/S) if 1≤ C/S ≤ 1.65
C-S-H †	CaH_2SiO_4	-8.16
Monosulfates	$3CaO.Al_2O_3.CaSO_4.12H_2O$	-29.4
Ettringite	$3CaO.Al_2O_3.3CaSO_4.26H_2O$	-44.0
Friedel's salt*	$3CaO.Al_2O_3.CaCl_2.12H_2O$	2.5
Hydroxy-AFm	$4CaO.Al_2O_3.13H_2O$	-25.4
Gypsum	$CaSO_4.2H_2O$	-4.58
Thaumasite	$2CaO.2SiO_2.2CaSO_4.2CaCO_3.26H_2O$	-44.7
Calcite	$CaCO_3$	-8.48
Monocarboaluminate	$3CaO.Al_2O_3.\ CaCO_3.11H_2O$	-31.47

† $C\text{-}S\text{-}H \rightarrow 0.65\ Ca(OH)_2 + CaH_2SiO_4$

* Ionic exchange mechanism: $Monosulfate + 2Cl^- \leftrightarrow Friedel's\ salt + SO_4^{2-}$

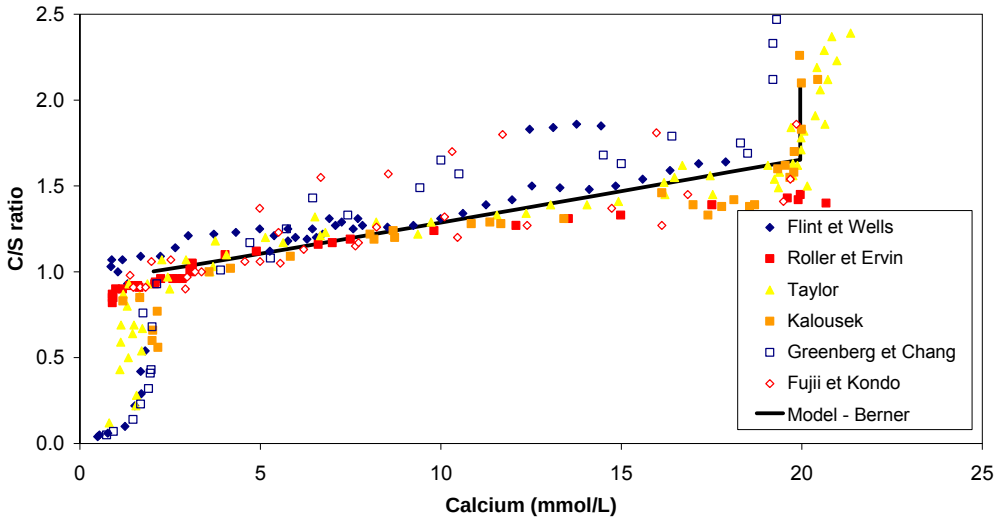

Figure 3 – C/S vs. calcium relationship for C-S-H

4.2. Space Discretization

In order to limit the calculation time as much as possible, and given the large size of the domain considered, a variable density finite element method (FEM) meshes are used for all the simulations. Specific functions were devised for the CBP project to generate good quality meshes that allow convergence at a reasonable CPU-time cost. To generate the mesh, the space $0 \leq \xi \leq 1$ is evenly divided into N nodes:

$$\xi = \frac{n - n_o}{N - 1} \tag{2}$$

where n is the node number and n_o is the number of the first node in the mesh (usually equal to one). For a mesh refined near x=0, the positions of the nodes in the mesh are given by:

$$x = x_o + L\xi^m \tag{3}$$

where x_o is the position of the first node in the mesh, L is the total length of the domain and $m \geq 1$ is called the mesh density factor. A mesh density factor of one gives a uniformly distributed mesh. Similar to equation (3), if the mesh is refined near x=L, the positions of the nodes are given by:

$$x = x_o + L\left(1 - (1 - \xi)^m\right) \tag{4}$$

For a mesh refined at both extremities, the same approach is used, only this time two different functions are specified. For each half-space $\xi \leq 0.5$ and $0.5 \leq \xi \leq 1$, the positions of the nodes are given by:

$$x = x_o + \frac{L}{2}(2\xi)^m \quad \text{for } \xi \leq 0.5 \tag{5}$$

$$x = x_o + \frac{L}{2} + \frac{L}{2}\left(1 - (2 - 2\xi)^m\right) \quad \text{for } 0.5 \leq \xi \leq 1 \tag{6}$$

For example, the mesh used for the concrete layer in every simulation[3] is shown on Figure 4. It is composed of 51 nodes (50 elements) and the mesh density factor is 1.35.

[3] Except for the simulations where different mesh densities are compared.

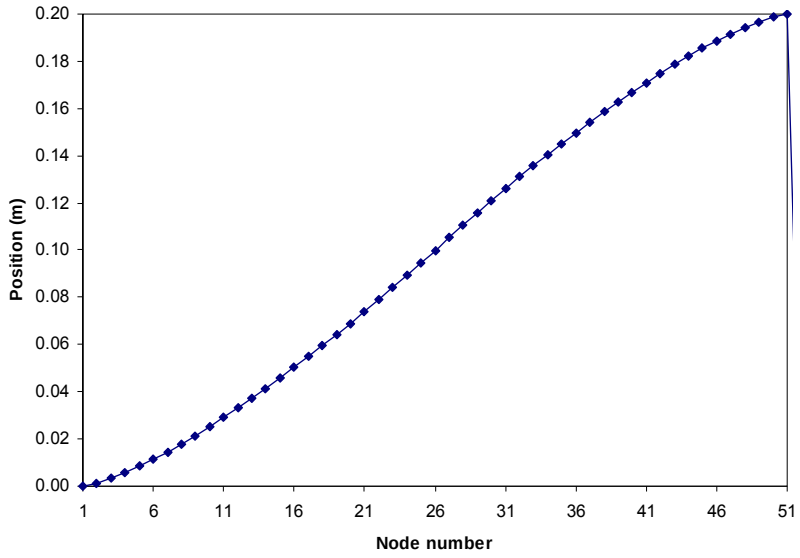

Figure 4 – Node distribution in the FE mesh of the concrete layer

4.3. Time Discretization

An adaptive time stepping scheme is used to gradually increase the time step up to 50 days. In all simulations, the initial time step is 5000 sec. When the norm of the numerical solution of the transport equations at the first iteration of a time step is lower than $5 \cdot 10^{-3}$, the time step is increased by a factor of 1.5, until a maximum time step of 50 days (4,320,000 sec.) is reached. The value of 50 days has been selected arbitrarily. Additional simulations would be needed to verify that this value can be increased, which would contribute to lower the calculation time.

The only simulation that required another set of time stepping parameters was when 3 m of soil and 3 m of Saltstone with 20 cm of concrete in between were simulated. This represented the largest domain simulated for this report. In this case, the threshold value that triggered a change in time step was set at $2 \cdot 10^{-3}$ and the time step were increased by a factor of 1.25.

4.4. Boundary Conditions

In all simulations, a null flux boundary condition was applied for the ionic species at the end of the Saltstone material (x=L). At the other end of the domain (x=0), the concentrations of all species are set to zero (Dirichlet boundary conditions), whether soil is present or not.

Temperature starts at 23 °C. An exchange flux condition $q = h(T - T_\infty)$ is imposed at x=0 and x=L, with h=5 W/m^2/°C and T_∞=15 °C. This causes a rapid drop in temperature in all layers so that the temperature can be considered uniform for the duration of the simulations.

The relative humidity is set to 1.0 at both ends of the FE mesh to enforce the saturated boundary conditions.

5.0 SIMULATION RESULTS

5.1. Summary

The simulations performed for Task 7 are summarized in the following table.

Table 8 – Task 7 simulation summary

Series	Simulation name	Concrete	Saltstone Thickness (cm)	Soil Thickness (cm)
Effect of the Saltstone thickness	Vault2-Saltstone-01	Vault 2	50	N/A
	Vault2-Saltstone-02	Vault 2	100	N/A
	Vault2-Saltstone-04	Vault 2	200	N/A
	Vault2-Saltstone-05	Vault 2	300	N/A
	Vault2-Saltstone-08	Vault 2	500	N/A
Effect of soil thickness	Vault2-Saltstone-Soil-01	Vault 2	300	100
	Vault2-Saltstone-Soil-02	Vault 2	300	300
Effect of mesh density	Vault2-Saltstone-06	Vault 2	300	N/A
	Vault2-Saltstone-07	Vault 2	300	N/A
Effect of concrete properties	Vault14-Saltstone-01	Vault 1/4	300	N/A
Effect of Saltstone initial mineral assemblage	Vault2-Saltstone-09	Vault 2	300	N/A

5.2. Effect of Saltstone Thickness

The first series of simulations was performed to investigate the impact of the Saltstone thickness on the kinetics of the penetration of the ettringite front into the concrete barrier. The objective was to find the thickness needed to simulate a semi-infinite domain. Not considering enough Saltstone would affect the degradation kinetics by underestimating the amount of sulfate in contact with the barrier. On the contrary, considering a Saltstone thickness that is unnecessarily too large would result in a large calculation time.

As shown on Table 8, the simulations were performed only based on the Vault 2 concrete mixture. This is because both concrete mixtures exhibit similar transport properties. However, the effect of the waste form layer thickness would vary from one material the other, as it is the barrier transport properties that limit the flux of contaminant from the slurry to the soil.

The simulations were performed for 50, 100, 200, 300, and 500 cm of Saltstone. The impact of the thickness was assessed by looking at the concentrations of Na^+, NO_2^-, NO_3^- and SO_4^{2-} at $x=L$. If the domain is large enough, it is expected that the concentrations after 10,000 years at $x=L$ would not have changed from their initial values. Results for 50, 300 and 500 cm of Saltstone are shown on Figure 5. With 50 cm of Saltstone, the sulfate concentration starts dropping after 200 years. Similar results were obtained for 100 and 200 cm of Saltstone. For 300 cm of Saltstone (Figure 5b), the concentrations in sodium, nitrite and nitrate are almost constant over 10,000 years. The concentration in sulfate drops after 3,000 years from 75 mmol/L to 40 mmol/L. Finally the simulation made with 500 cm of Saltstone (Figure 5c) was very close to a semi-infinite condition as the concentrations are only showing a very slight drop after 10,000 years.

This indicates that at least 5 m of Saltstone are needed to simulate the long term durability of the concrete barrier. But interestingly, the sulfate concentration at the concrete/ Saltstone interface is very similar for 300 cm and 500 cm, as shown on Figure 6. According to this figure, using 3 m of Saltstone to simulate the durability of the concrete barrier over 10,000 years is large enough. This plot also provides information on the sulfate concentration to be imposed at the concrete surface in a simplified performance assessment. Fitting the sulfate vs. time data with a Weibull-type function for 3 m of Saltstone (see Figure 7) gives:

$$[\mathrm{SO}_4^{2-}] = a - be^{-ct^d} \tag{7}$$

where a = 56.132271, b = 70.963039, c = 21.967298, d = -0.44279133 and t is the time in years.

The solid phase content in the concrete barrier predicted by the simulation with 3 m of Saltstone is illustrated in Figure 8 after 5000 years. The results show that ettringite forms in the concrete as a result of the sulfate diffusion from the Saltstone. However, other deleterious phases such as gypsum and thaumasite were not predicted by STADIUM®. Also, the amount of ettringite formed is not very important because alumina is shared with monocarboaluminate. The porosity profile on Figure 9 shows that ettringite does not occupy a large volume and would likely not cause damage to the material. However, the dissolution of phases near the concrete surface (x=0) due to leaching corresponds to an important increase in porosity.

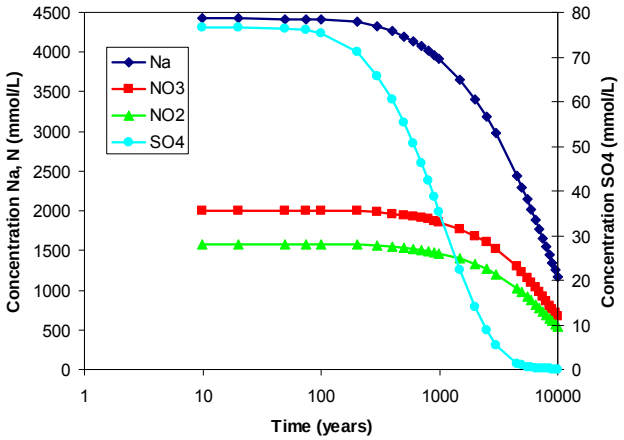

a) 50 cm of Saltstone

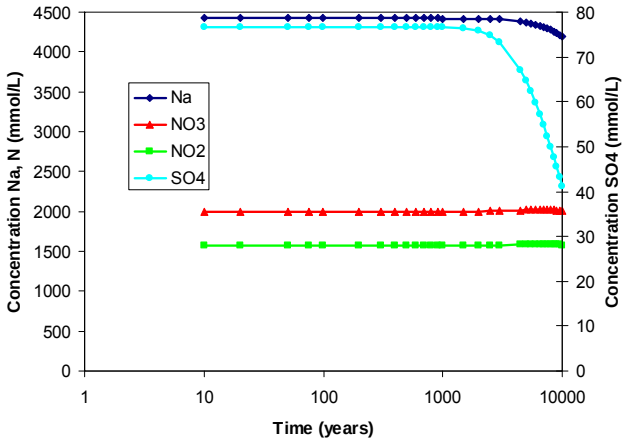

b) 300 cm of Saltstone

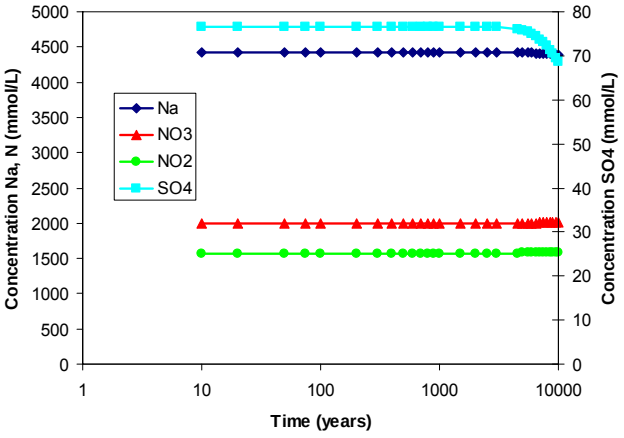

c) 500 cm of Saltstone

Figure 5 – Concentration of species Na, NO3, NO2 and SO4 at the end of the Saltstone domain

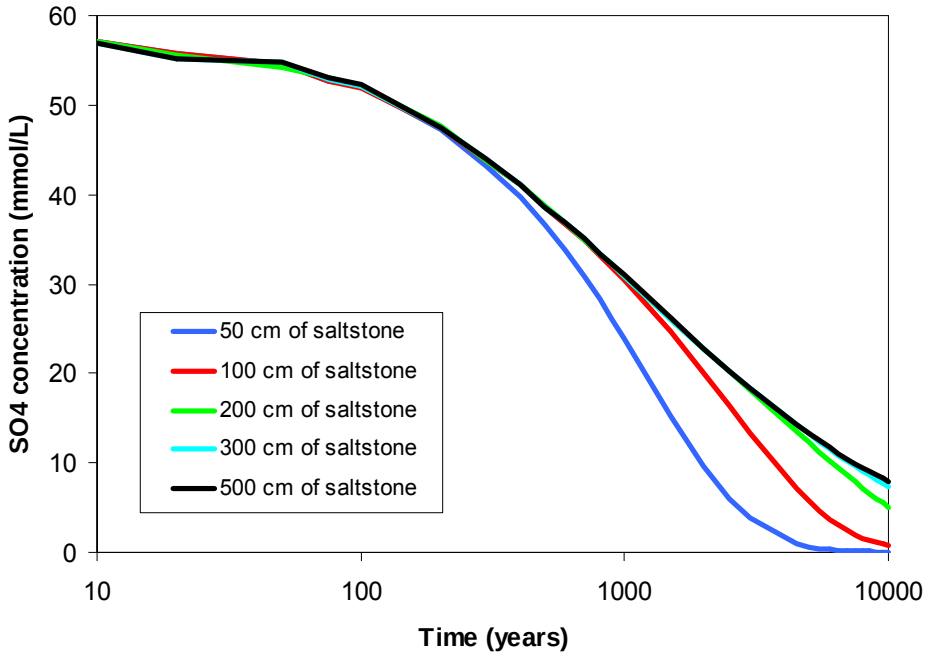

Figure 6 – Sulfate concentration at the concrete/Saltstone interface

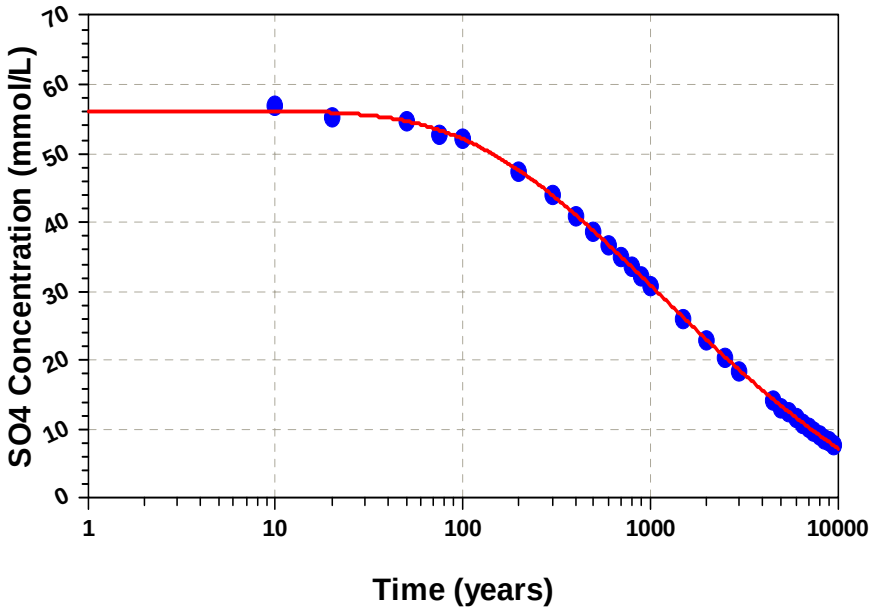

Figure 7 – Fitting of the SO4 concentration at the Saltstone/concrete interface for 3 m of Saltstone

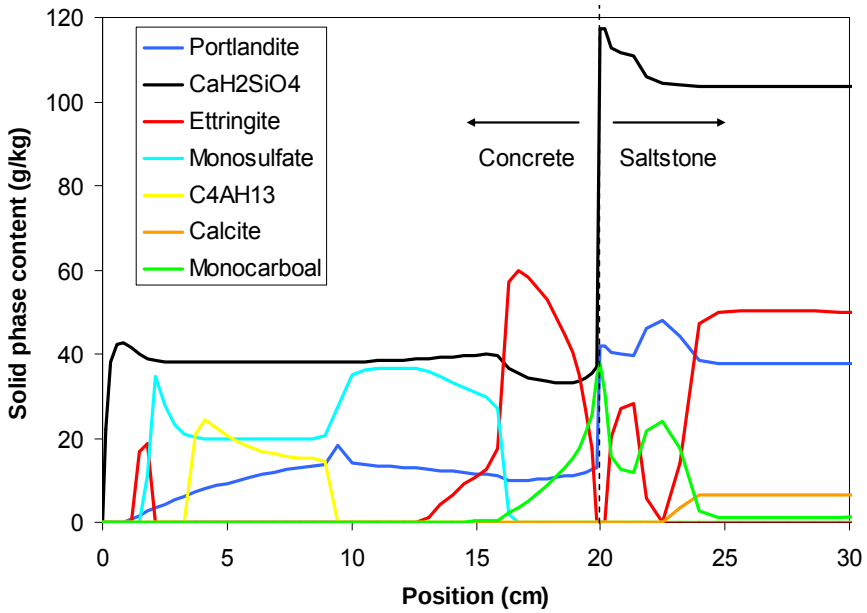

Figure 8 - Solid phase distribution in the Vault 2 concrete after 5,000 years

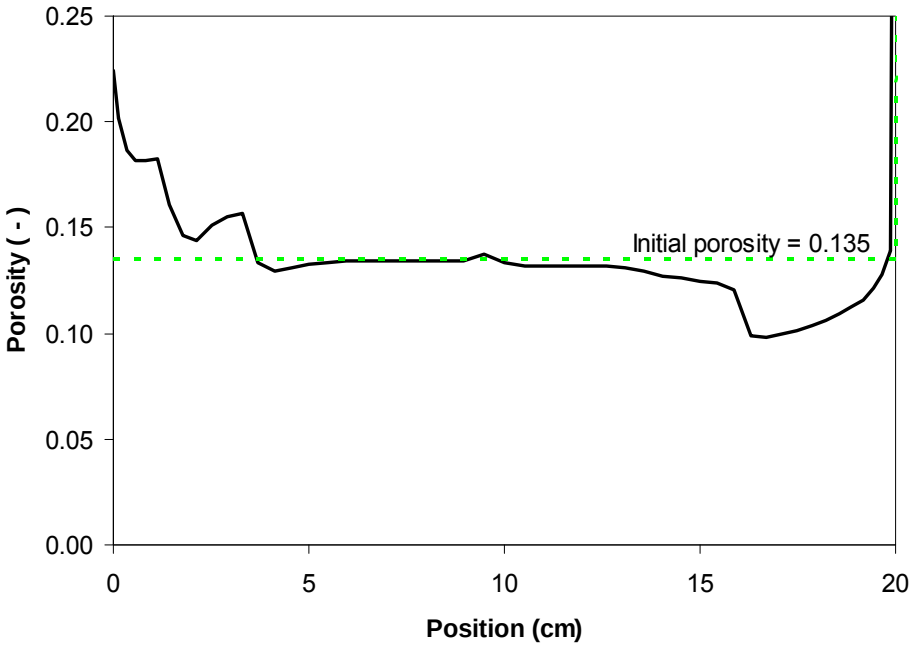

Figure 9 – Porosity profile in the concrete layer associated with the phase distribution of Figure 8

The kinetics of the ettringite front penetration that starts at the Saltstone/concrete interface is illustrated on Figure 10. The position of the front was estimated by the position where the ettringite level reaches 30 g/kg. The numerical results were fitted to the function[4]:

$$y = ab^t t^c \tag{8}$$

with y representing the ettringite front position (cm), t is the time (years) and the fitting parameters given by: a=0.10051665, b=0.99997865, c=0.44623361.

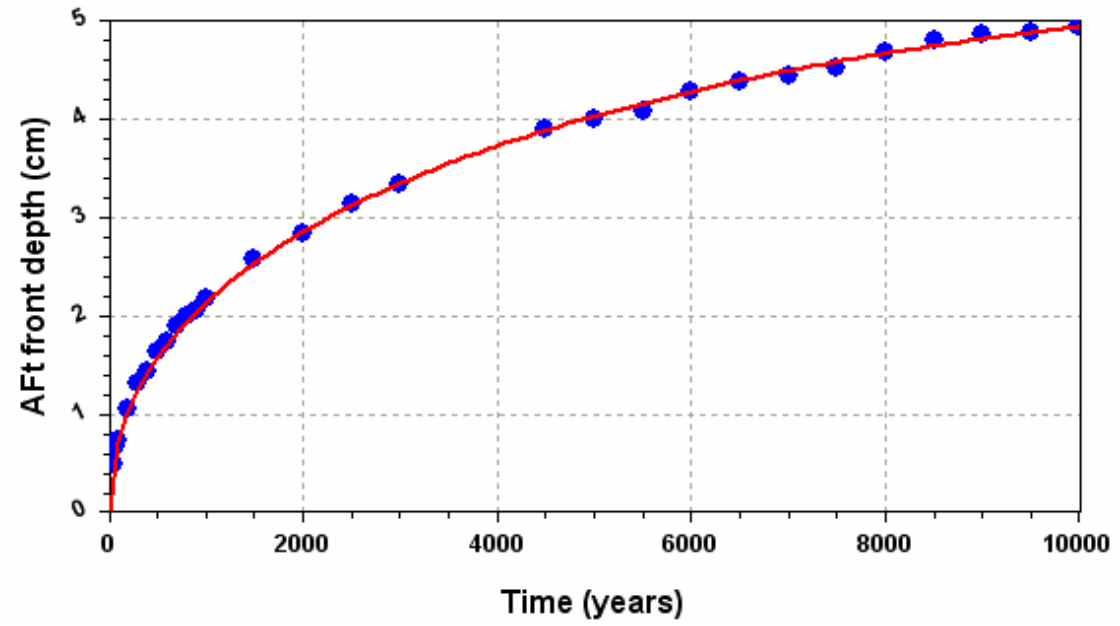

Figure 10 – Ettringite front depth in concrete vs. time

A similar analysis was performed to assess the kinetics of the C-S-H decalcification occurring at x=0, where the concrete is in contact with the soil. As mentioned previously, the calculations in this series were based on the assumption of a high-velocity flow field in the soil, as illustrated on Figure 2a. The concentrations were set to zero at the soil/concrete interface. The portlandite illustrated on Figure 8 corresponds to the actual portlandite plus the contribution from a fraction of the C-S-H according to Berner's approach (see the section on chemical data). The complete dissolution of portlandite indicates that the real portlandite is dissolved and that the C-S-H is decalcified. The remaining C-S-H corresponds to the CaH_2SiO_4 portion and offers no significant mechanical resistance. For the purpose of the analysis, the decalcification front corresponds to the position where the portlandite content drops to 3 g/kg. The results are given in Figure 11. The data were fitted to equation (8) with the parameters: a=0.084722747, b=1.000008, c=0.36636674.

[4] The function does not fit the trend after 10,000 years. For extrapolation, the function $y = 0.1041t^{0.4327}$ offers a better fit.

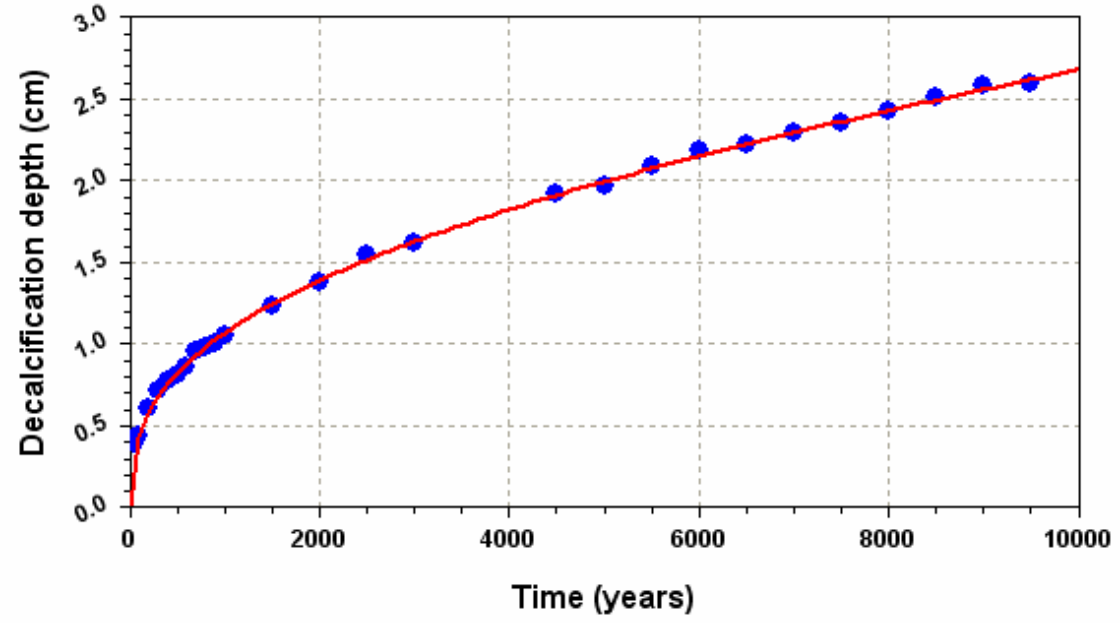

Figure 11 – Depth of the decalcification front starting at x=0

5.3. Effect of Soil Thickness

The simulations in the previous section were made under the assumption that the water velocity field at the soil/concrete interface was large enough to allow setting the concentrations to zero at this boundary. It means that the diffusion in the soil is neglected. As illustrated in Figure 2, weaker flow field would result in a diffusion zone in the soil where the species leaching from the concrete would have a non-zero concentration.

The objective of this simulation series is to estimate the impact of soil diffusion on the durability of the concrete barrier. The base case corresponds to the simulation with concrete and 300 cm of Saltstone (simulation *Vault2-Saltstone-05*, see Table 8). The results of this simulation will be compared to simulation results obtained with 1 m and 3 m of soil, corresponding to the cases illustrated in Figure 2b and Figure 2c, respectively. For these two simulations, the species concentrations were set to zero at the beginning of the soil domain, which corresponds to x=0 in Figure 1a. This case was selected to emphasize the decalcification resistance of the barrier. Other cases with sulfate or carbonate in the groundwater could also be modeled with STADIUM®.

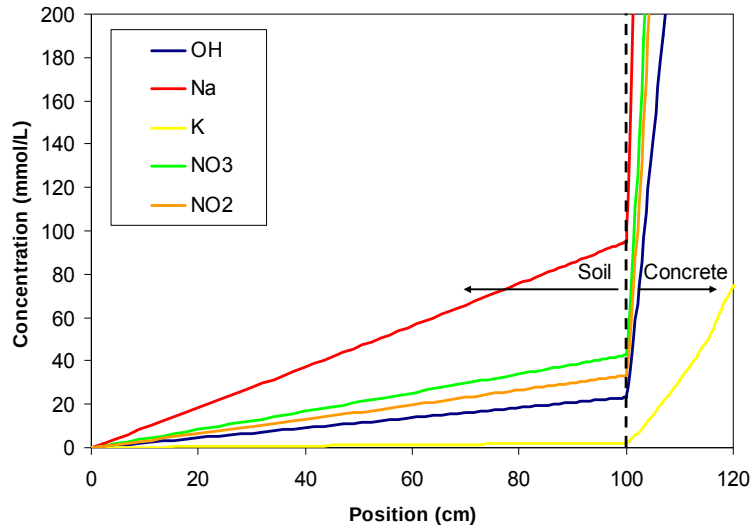

a) 1-m soil layer

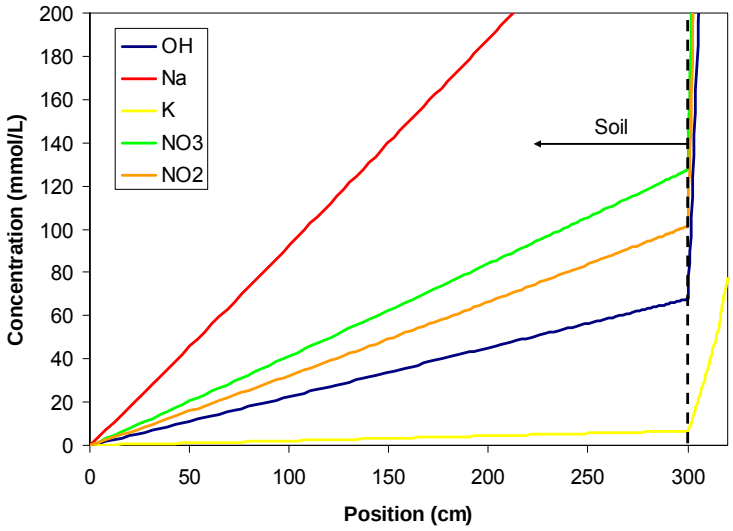

b) 3-m soil layer

Figure 12 – Concentration profiles of selected species in the soil layer after 5,000 years

The ionic species distribution in the soil layer is illustrated on Figure 12. Figures 12a and 12b show a sharp drop in concentration at the soil/concrete interface due to the high diffusion rate in the soil layer. Figure 12a shows that considering 100 cm of high tortuosity soil is very similar to imposing a zero concentration on the concrete surface. Extending the soil layer to 3 m raises the concentration levels at the interface.

The impact on degradation kinetics is illustrated in the next two figures. Figure 13 illustrates the effect of the soil layer thickness on the rate of penetration of the ettringite front in the concrete layer. STADIUM® does not predict any significant effect of the soil layer thickness.

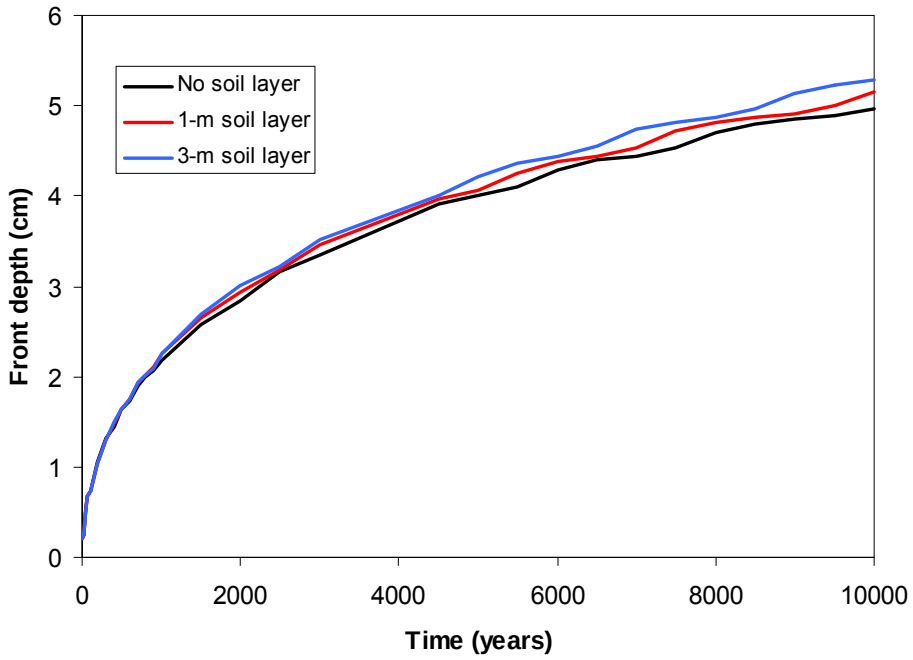

Figure 13 – Ettringite front depth in concrete for different soil layers

The situation is different in the case of the decalcification occurring at the soil/concrete interface. The presence of soil slows the drop of pH on the concrete surface, which prevents decalcification from starting. As shown in Figure 14, the decalcification depth predicted by STADIUM® is two times less when 1 m of soil is considered in the simulations. When 3 m of soil is modeled, decalcification does not occur. The mineral content distribution shown in Figure 15 shows that portlandite is still present at the soil/concrete interface after 10,000 years.

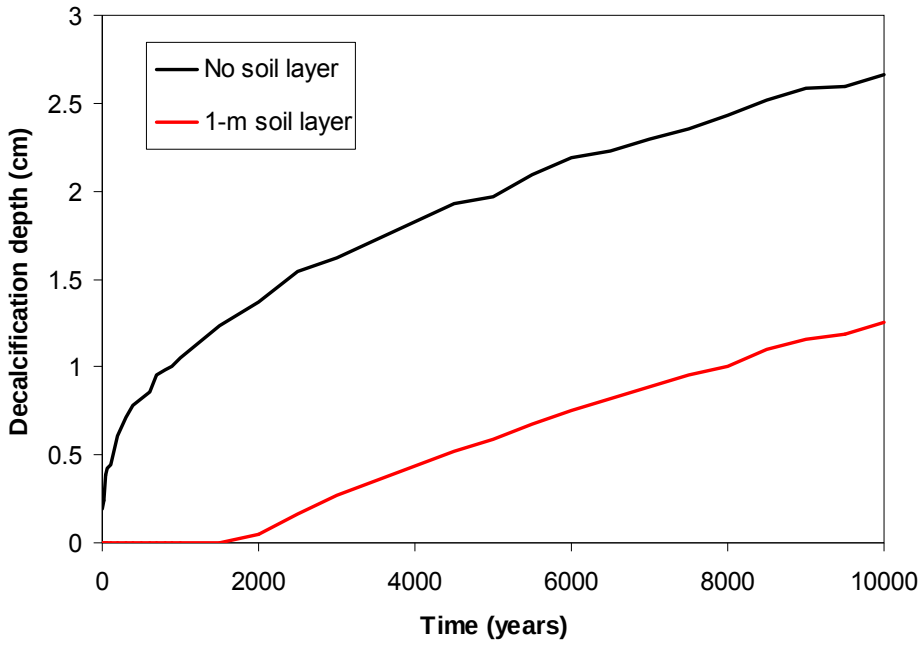

Figure 14 – Decalcification depth vs. soil thickness

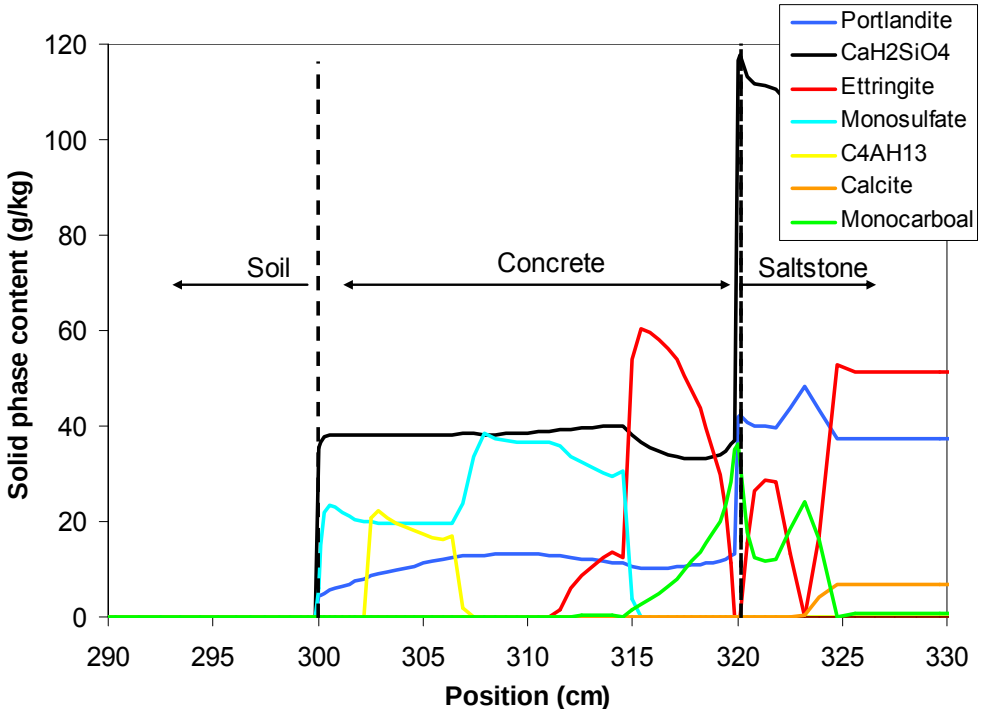

Figure 15 – Solid phase distribution after 10,000 years with 3 m of soil

5.4. Effect of Mesh Density

Simulations were performed to assess the quality of the numerical solution by comparing the effect of different mesh densities. The test case corresponds to simulation *Vault2-Saltstone-05*, where 3 m of Saltstone and no soil layer were modeled. This simulation was performed with 50 elements in the concrete layer (mesh factor=1.35, see Figure 4) with mesh refinement at both ends, and 120 elements in the Saltstone layer (mesh factor=1.6) with mesh refinement only at the concrete/Saltstone interface.

The simulation of the base case is compared to results obtained with ±20% elements using the same mesh factors. The simulations results for the three different meshes proved nearly identical. This is illustrated in Figure 16, which shows the ettringite profile in the concrete layer after 10,000 years.

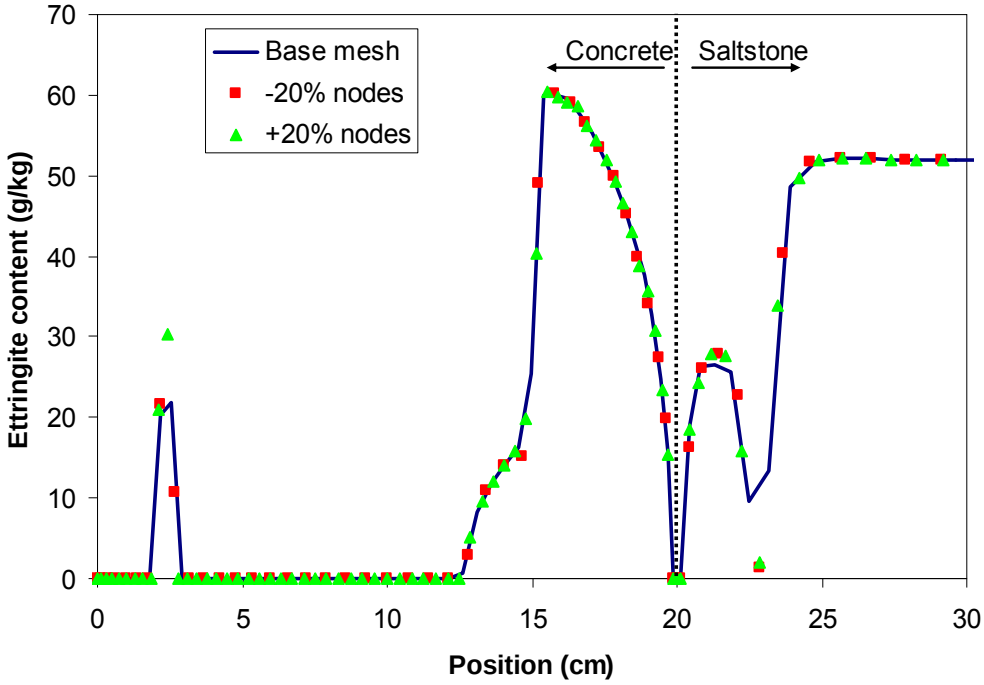

Figure 16 – Comparison of ettringite profiles for different mesh densities

However, the mesh density has a strong impact on calculation time. The calculation times for the three cases illustrated on Figure 16 are listed in Table 9. These numbers do not offer a strict comparison of the calculation time because they were not all performed on the same computer[5]. But even in that case, the reduction in the number of elements shows a significant decrease in calculation time. This indicated that a systematic investigation to determine the optimal mesh density would be worthwhile, especially in the context of a statistical analysis of the concrete barrier durability.

[5] Most simulations were performed on either a Windows XP SP3 HP Workstation with a Pentium 4, 3.2 GHz, 1.5 GB of RAM or on a Windows XP SP3 HP Intel Xeon Workstation with 2 CPUs/3.06 GHz, 1GB of RAM.

Table 9 – Calculation time vs. mesh densities

Simulation	Total number of nodes	Calculation time (hours)
Base case – *Vault2-Saltstone-05*	171	30.5
-20% elements – *Vault2-Saltstone-06*	137	19.0
+20% elements – *Vault2-Saltstone-07*	205	33.8

5.5. Effect of Concrete Properties

The case with a 3-m layer of Saltstone and without a soil layer (*Vault2-Saltstone-05*) was simulated again with the Vault 1/4 concrete properties. Both materials are high performance concretes having low tortuosity (see Table 2) and were prepared with a high quantity of binder. The Vault 2 material has a lower tortuosity and is thus expected to perform better, meaning less ettringite penetration and C-S-H decalcification. However, the chemical composition of cementitious materials used to prepare both mixtures is different and may impact the long-term durability.

The solid phase distribution in the Vault 1/4 concrete after 5,000 years of exposure to Saltstone is shown on Figure 17. Similar to the Vault 2 mixture, the exposure to Saltstone induced the penetration of an ettringite front but gypsum and thaumasite are not predicted by STADIUM® even though they were included in the calculations as possible precipitates. Overall, the mineral phase distribution predicted by the model for the Vault 1/4 concrete is very similar to the phase predicted for the Vault 2 mixture (see Figure 8). Consequently, the porosity profiles for both materials are very similar (Figure 9 and Figure 18). It can be noted that since the total amount of sulfur and alumina is higher in the Vault 1/4 concrete, the height of the ettringite front is higher, which translates into a more pronounced drop in porosity near the concrete/Saltstone interface.

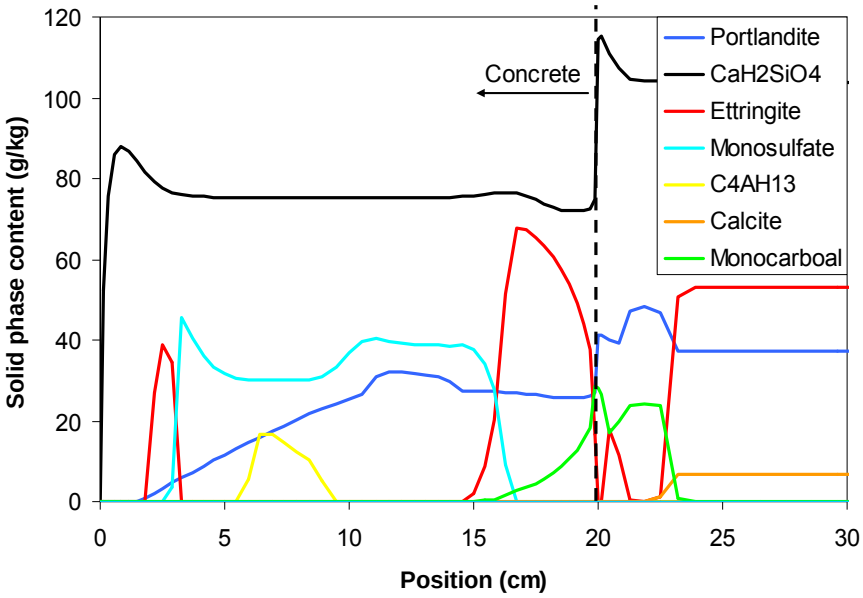

Figure 17 – Solid phase distribution in the Vault 1/4 concrete after 5,000 years

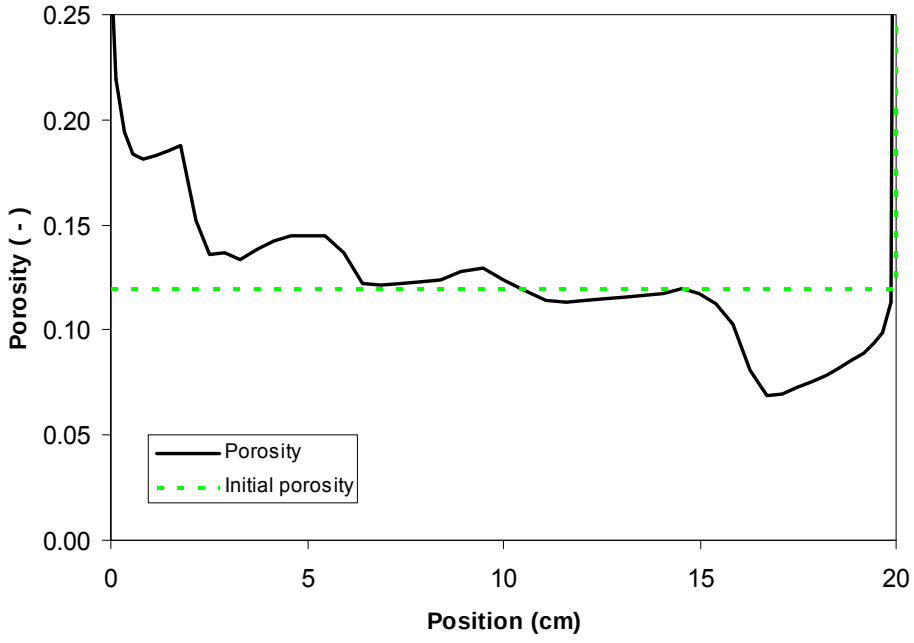

Figure 18 – Porosity profile in the concrete layer associated with the phase distribution of Figure 17

The front penetration kinetics for both materials is compared in Figure 19. The results indicate that initially, the ettringite front is propagating more rapidly into the Vault 1/4 mixture, most probably because it has a higher tortuosity than the Vault 2 mixture. However, the penetration kinetics decreases gradually. This can be

attributed to the pore blocking effect induced by the formation of ettringite, which is more important than in the Vault 2 mixture because of the presence of more sulfur and alumina in the binders.

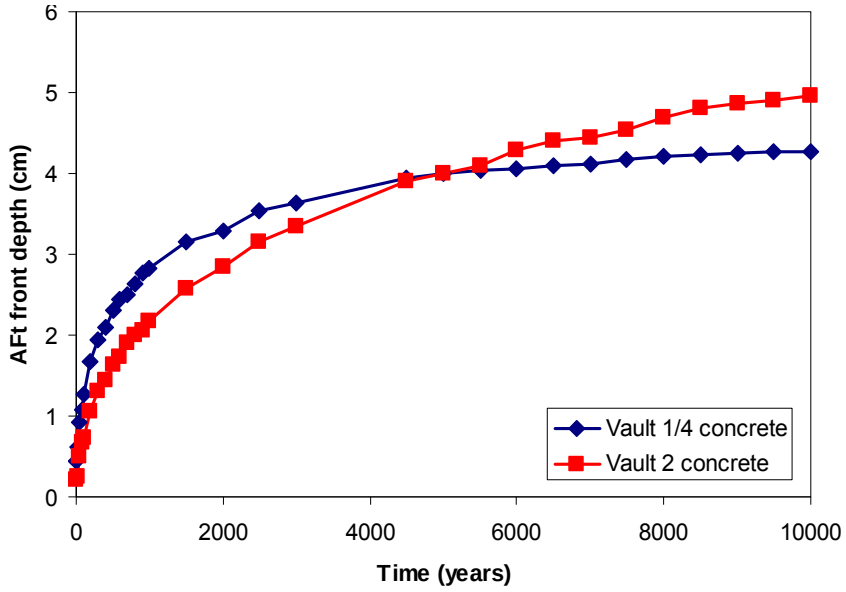

Figure 19 – Comparison of the AFt front kinetics for the Vault 2 and Vault 1/4 mixtures

The pore blocking effect is not present at the other end of the concrete layer, where concrete is being decalcified. In that case, the driving mechanism is diffusion and the decalcification process is mainly influenced by the tortuosity. This results in more important decalcification kinetics for the Vault 1/4 mixture, as shown in Figure 20.

Again using the function $y=ab^t t^c$, the ettringite front kinetics is fitted with parameters: a=0.27340499, b=0.99995958, and c=0.34022181. The parameters for the decalcification kinetics are: a=0.051299116, b=0.99999951, and c=0.45721395.

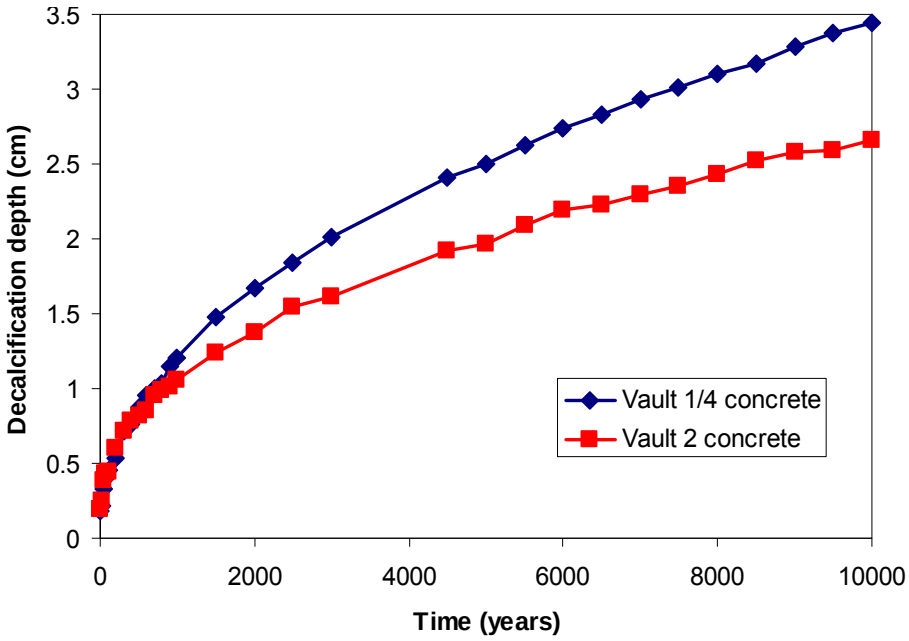

Figure 20 – Comparison of the depth of decalcification for the two concrete mixtures

5.6. Effect of Saltstone Initial Mineral Assemblage

It was noted during the early rounds of simulations that, depending on the minerals initially present in the Saltstone, it was possible to have the sulfate enter the concrete barrier without forming ettringite. The last series of results was performed to illustrate this. If it is assumed that the initial assemblage is C-S-H, ettringite and monocarboaluminate, instead of C-S-H, ettringite and calcite, the procedures detailed in the section on the Saltstone properties yields the initial assemblage and pore solution listed in Table 10. Compared to the previous assemblage, calcite is not present in the Saltstone and more monocarboaluminate is found in the Saltstone. Also, monosulfate is present in the paste.

This set of minerals is used as input data to simulate the Vault 2 concrete barrier in contact with 3 m of Saltstone. As seen in Figure 21, the alteration to the concrete microstructure near the concrete/Saltstone interface is very different than what was predicted by STADIUM® with the former Saltstone (Figure 8). The most striking difference is the absence of an ettringite front in the concrete barrier. Interestingly, it is also noted that no carbonate-based phase is precipitated in the concrete.

At the other end of the concrete layer, decalcification is predicted by the model. In this case, the initial mineral assemblage in Saltstone has little impact on the degradation kinetics.

Table 10– Initial mineral assemblage in the Saltstone paste

Phases	Amount	
Minerals	($g/kg_{Saltstone}$)	
C-S-H	117.3	
Portlandite	3.4	
Ettringite	30.1	
Monosulfate	11.3	
Monocarboaluminate	39.2	
Calcite	0.0	
Pore Solution	(mmol/L)	Act. coef.
OH^-	766.0	0.9298
Na^+	4420.0	0.4400
K^+	120.0	0.3222
SO_4^{2-}	82.0	0.0337
Ca^{2+}	0.3	0.0442
$Al(OH)_4^-$	0.4	0.6992
Cl^-	9.0	0.8156
$H_2SiO_4^{2-}$	12.5	0.0377
NO_3^-	2000.0	0.3978
NO_2^-	1575.0	0.3276
CO_3^{2-}	0.4	0.0617

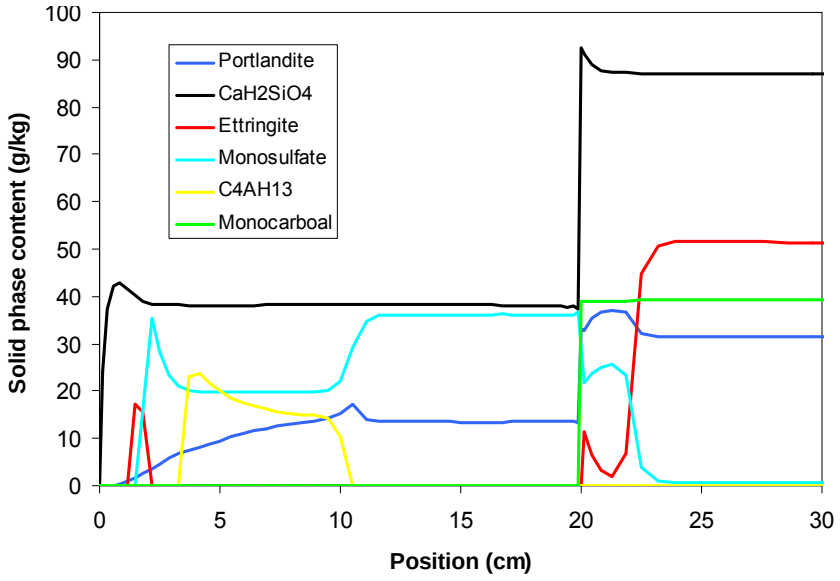

Figure 21 – Solid phase distribution in the Vault 2 concrete after 5,000 years based on the new mineral assemblage in Saltstone

6.0 CONCLUSION

The calculations made in this report showed the capacity of STADIUM® in handling complex multilayer cases to predict the durability of concrete barriers in contact with sulfate bearing Saltstone-type material.

Some results already provide guidance on performance assessment simulations to estimate the durability of the concrete barrier. For instance, the thickness of the Saltstone layer considered in the simulation has a significant impact on the model prediction. The results obtained in this report indicate that at least 3 m of salt waste material should be used to simulate the long term durability of the barrier.

At the soil/concrete barrier interface, the situation is different. The simulations indicated that the thickness of the soil layer considered has very little impact on the kinetics of the ettringite front penetration that starts at the Saltstone/concrete boundary. The soil layer does have an influence on the rate of decalcification of C-S-H at the soil/concrete barrier interface. But since the most critical case corresponds to simulations without a soil layer, it is recommended that this layer be neglected. This would have the added benefit of reducing the calculation time.

However, the most important result concerns the influence of different mineral assemblages in the Saltstone mixture. The second set of minerals used for the simulations did not initiate the penetration of an ettringite front in the concrete barrier despite the high sulfate concentration in the pore solution. The absence of ettringite means that the concrete is not subject to sulfate attack and could prove highly durable for an extensive period of time. This surprising result emphasizes the need for experimental research work in order to have a better understanding of the complex interaction between the salt waste material and the concrete barrier.

7.0 REFERENCES

Maltais Y., Samson E., Marchand J. (2004) Predicting the durability of Portland cement systems in aggressive environments – Laboratory validation, Cement and Concrete Research 34, 1579-1589.

SIMCO Technologies Inc. (2009a) Report Tasks 2 & 4 – Experimental Results from Vault Concretes, Subcontract no. AC48992N, July 2009.

SIMCO Technologies Inc. (2009b) Report Task 6 – Characterization of a Saltstone mixture, Subcontract no. AC48992N, July 2009.

APPENDIX A – MINERAL PHASE CALCULATIONS

Methodology

1. Basic principles

The methodology developed at SIMCO Technologies Inc. to estimate the initial mineral phase content in hydrated cement pastes is based on the mass conservation of the calcium, silica, alumina, and sulfur that is available to form hydration products.

The main hypotheses of the calculation are listed in the following paragraphs:

- It is assumed that SO_3 in cement and supplementary cementitious admixtures is highly soluble and is almost totally available to form hydration products. Accordingly, 90% of the total sulfur content will be found in monosulfate (AFm) and ettringite (AFt). The remaining 10% is not available, due to possible substitution in C-S-H.
- Depending on the amount of Al and S available, different assemblages will be formed. If there is enough Al to transform all S into monosulfate, the initial assemblage will contain monosulfate and hydroxy-AFm. The hydroxy-AFm phase is based on the composition and molar mass of C_4AH_{13} but should be considered more generally as AFm-OH. If there is not enough Al to transform all available S into monosulfate, the amount of S and Al available will compete to form monosulfate and ettringite.
- The calculation of the C-S-H content is based on a C/S ratio of 1.65 according to the composition: C-S-H = CaH_2SiO_4 + 0.65 $Ca(OH)_2$
- It is known that a significant portion of alumina can be substituted in C-S-H. On the other hand, iron is reactive and can contribute to the formation of AFm phases. Accordingly, the content of Al is calculated on the basis of the cement and SCM compositions and their respective hydration level. However, this amount can be modified by a factor to account for the fact that a given cement can be more reactive than another with a similar Al level. This is evidenced in chloride ponding test results that show a different binding level near the material surface.

The calculation steps are provided in the next sections.

2. Calculation of the main components

The first step consists in calculating the total amount of Ca, Al, S and Si. Given the chemical composition of the cement (C) and different SCM (1, 2, 3) in mass percentages of CaO, SiO_2, Al_2O_3 and SO_3, their respective hydration level (□, [0-1]), and the mixture proportions in kg/m^3, the calculations are [g/kg$_{material}$]:

- Ca_{tot} = $[10\ \alpha_C\ [CaO_C]\ [C]/\rho +$
  $10\ \alpha_{SCM1}\ [CaO_{SCM1}]\ [SCM_1]/\rho +$
  $10\ \alpha_{SCM2}\ [CaO_{SCM2}]\ [SCM_2]/\rho$

$10\ \alpha_{SCM3}\ [CaO_{SCM3}]\ [SCM_3]/\rho\ ]\ (M_{Ca}/M_{CaO})$

- Si_{tot} = $[10\ \alpha_C\ [SiO_{2,C}]\ [C]/\rho$ +
  $10\ \alpha_{SCM1}\ [SiO_{2,SCM1}]\ [SCM_1]/\rho$ +
  $10\ \alpha_{SCM2}\ [SiO_{2,SCM2}]\ [SCM_2]/\rho$
  $10\ \alpha_{SCM3}\ [SiO_{2,SCM3}]\ [SCM_3]/\rho\ ]\ (M_{Si}/M_{SiO2})$

- Al_{tot} = $[10\ \alpha_C\ [Al_2O_{3,C}]\ [C]/\rho$ +
  $10\ \alpha_{SCM1}\ [Al_2O_{3,SCM1}]\ [SCM_1]/\rho$ +
  $10\ \alpha_{SCM2}\ [Al_2O_{3,SCM2}]\ [SCM_2]/\rho$
  $10\ \alpha_{SCM3}\ [Al_2O_{3,SCM3}]\ [SCM_3]/\rho\ ]\ (2\ M_{Al}/M_{Al2O3})$x (Al reaction factor)

- S_{tot} = $[10$ x $0.9\ [SO_{3,C}]\ [C]/\rho$ +
  10 x $0.9\ [SO_{3,SCM1}]\ [SCM_1]/\rho$ +
  10 x $0.9\ [SO_{3,SCM2}]\ [SCM_2]/\rho$
  10 x $0.9\ [SO_{3,SCM3}]\ [SCM_3]/\rho\ ]\ (M_S/M_{SO3})$

where M_i is the molar mass of component i. The molar masses [g/mol] are given by:

M_{Ca}: 40.08	M_{CaO}: 56.0794
M_{Si}: 28.086	M_{SiO2}: 60.0848
M_{Al}: 26.98154	M_{Al2O3}: 101.9613
M_S: 32.06	M_{SO3}: 80.0582
M_{AFm}: 622.5195	M_{CH}: 74.0946
M_{AFt}: 1255.0987	M_{CSH}: 182.34089
M_{AFm-OH}: 560.4765	

3. Determination of the Al/S assemblage

The amount of Al_{tot} and S_{tot} determines the presence of AFm-OH or ettringite (AFt):

- if ($S_{tot}\ M_{AFm} / M_S < Al_{tot}\ M_{AFm} / (2\ M_{Al})$)

  $AFm = S_{tot}\ M_{AFm} / M_S$

  $Al_{tot} = Al_{tot} - 2\ AFm\ M_{Al}/M_{AFm}$ (remaining amount of Al for AFm-OH)

  $AFm\text{-}OH = Al_{tot}\ M_{AFm\text{-}OH} / (2\ M_{Al})$

- else, a system of 2 equations and 2 unknowns is solved to determine the amount of ettringite and monosulfate:

  $AFt = -0.25\ M_{AFt}\ (Al_{tot} - 2\ M_{Al}\ S_{tot}/M_S)\ /M_{Al}$

  $AFm = 0.5\ M_{AFm}\ (Al_{tot} - 2\ M_{Al}\ AFt\ /\ M_{AFt}\ )\ /\ M_{Al}$

4. Calculation of the C-S-H content

The first step consists in calculating the amount of calcium remaining, which depends on the type of assemblage estimated at the previous step:

- if ($S_{tot} M_{AFm} / M_S < Al_{tot} M_{AFm} / (2 M_{Al})$)

$$Ca_{tot} = Ca_{tot} - 4\ AFm\ M_{Ca}/M_{AFm} - 4\ AFm\text{-}OH\ M_{Ca}/M_{AFm\text{-}OH}$$

- else

$$Ca_{tot} = Ca_{tot} - 4\ AFm\ M_{Ca}/M_{AFm} - 6\ AFt\ M_{Ca}/M_{AFt}$$

Knowing this, the amount of C-S-H is calculated, based on the amount of Si. If there is not enough calcium to use all Si, then all calcium is used and there will be no portlandite.

- if ($Si_{tot} M_{CSH} / M_{Si} < Ca_{tot} M_{CSH} / (1.65 M_{Ca})$)

$$CSH = Si_{tot}\ M_{CSH}/M_{Si}$$

- else

$$CSH = Ca_{tot}\ M_{CSH}/(1.65\ M_{Ca})$$

5. Calculation of the portlandite content

Finally, the final step consists in calculating the amount of portlandite based on the amount of calcium remaining:

- $Ca_{tot} = Ca_{tot} - 1.65\ CSH\ M_{Ca}/M_{CSH}$
- $CH = M_{CH}/M_{Ca}$

CBP Concrete Mixtures

PROJECT AND MATERIAL DESCRIPTION

CBP Task 7 - Vault 1/4 concrete initial mineral phase calculations

Mixture

		kg/m³	γ
Cement:	10	255.0	3.27
SCM #1	None	169.0	2.99
SCM #2	None	0.0	2.36
SCM #3	None	0.0	2.36
Water:		162.0	1.00
Fine aggregates:		691.0	2.68
Coarse aggregates:		1096.0	2.67

W/B ratio:	0.382	
Total binder:	424.0	kg/m³
% cement:	60.1	%
% SCM #1:	39.9	%
% SCM #2:	0.0	%
% SCM #3:	0.0	%
Saturated density:	2373.0	kg/m³
Paste volume:	0.297	
Binder density:	3158.4	kg/m³
Mixture volume:	0.965	m³

Bogue Analysis

C_3S:	56.60
C_2S	17.52
C_3A:	7.09
C_4AF:	10.65

Chemical composition

	Ciment	SCM #1	SCM #2	SCM #3
CaO (%):	64.30	35.80	0.00	0.00
SiO2 (%):	21.00	39.10	0.00	0.00
Al2O3 (%):	4.91	10.10	0.00	0.00
SO3 (%):	2.64	1.99	0.00	0.00
Fe2O3 (%):	3.50	0.36	0.00	0.00
Hydratation (0-1):	0.75	0.60	0.00	0.00
Al reaction factor:	0.75			

Solid phases

Material hydration (α):	0.69	
Portlandite:	2.2	g/kg
C-S-H:	102.1	g/kg
Monosulfates:	29.8	g/kg
C4AH13:	7.3	g/kg
Ettringite:	0.0	g/kg

C-S-H - Berner

Portlandite - total:	29.2	$g/kg_{matériau}$
CaH_2SiO_4:	75.1	$g/kg_{matériau}$

PROJECT AND MATERIAL DESCRIPTION

CBP Task 7 - Vault 2 concrete initial mineral phase calculations

Mixture

		kg/m³	γ
Cement:	50	121.0	3.29
SCM #1	Slag	162.0	2.99
SCM #2	Silica fume	27.0	2.32
SCM #3	Fly ash - F	95.0	2.36
Water:		154.0	1.00
Fine aggregates:		548.0	2.68
Coarse aggregates:		1111.0	2.67

W/B ratio:	0.380	
Total binder:	405.0	kg/m³
% cement:	29.9	%
% SCM #1:	40.0	%
% SCM #2:	6.7	%
% SCM #3:	23.5	%
Saturated density:	2218.0	kg/m³
Paste volume:	0.297	
Binder density:	2887.2	kg/m³
Mixture volume:	0.917	m³

Bogue Analysis

C_3S:	57.83
C_2S	16.02
C_3A:	3.58
C_4AF:	13.15

Chemical composition

	Ciment	SCM #1	SCM #2	SCM #3
CaO (%):	63.00	35.80	0.50	1.41
SiO2 (%):	20.80	39.10	96.60	53.10
Al2O3 (%):	4.11	10.10	0.21	28.40
SO3 (%):	2.36	1.99	0.05	0.05
Fe2O3 (%):	4.32	0.36	0.18	7.99
Hydratation (0-1):	0.75	0.50	0.90	0.20
Al reaction factor:	0.75			

Solid phases

Material hydration (α):	0.53	
Portlandite:	0.0	g/kg
C-S-H:	51.5	g/kg
Monosulfates:	19.4	g/kg
C4AH13:	14.8	g/kg
Ettringite:	0.0	g/kg

C-S-H - Berner

Portlandite - total:	13.6	$g/kg_{matériau}$
CaH_2SiO_4:	37.9	$g/kg_{matériau}$


U.S. DEPARTMENT OF
ENERGY


SRNL
SAVANNAH RIVER NATIONAL LABORATORY


CRESP


VANDERBILT
UNIVERSITY


UNITED STATES NUCLEAR REGULATORY COMMISSION


NIST
National Institute of
Standards and Technology


ECN


SIMCO
Technologies inc.